Journal of Soils and Sediments
https://doi.org/10.1007/s11368-025-04046-2

SOILS, SEC 2 • GLOBAL CHANGE, ENVIRONMENTAL RISK ASSESSMENT, SUSTAINABLE LAND USE • RESEARCH ARTICLE

# Study of the pyrolysis characteristics and soil amendment potential of palm mesocarp fiber, sago fiber coarse, and sago trunk bark in Malaysia

Kah Ho Yeong[1,2] · Tao Liu[1,2] · Lee Tung Tan[4] · Jiuan Jing Chew[4] · Yin Wang[1,3]

Received: 21 February 2025 / Accepted: 8 May 2025


## Abstract

**Purpose** Oil palm, sago, and coconut are key economic crops in Malaysia, but their processing generates large amounts of biomass waste. Pyrolyzing these wastes into biochar offers a sustainable solution, yet the pyrolysis characteristics and soil amendment potential of palm mesocarp fiber (PMF), sago fiber coarse (SFC), and sago trunk bark (STB) remain underexplored. This study investigates the physicochemical and pyrolysis characteristics of PMF, SFC, and STB at varying pyrolysis temperatures (300–700 °C), and evaluates the potential of the derived biochars on soil fertility and paddy growth.

**Methods** PMF, SFC, STB, and coconut shell (CS) were pyrolyzed at 300–700 °C and characterized for elemental composition, specific surface area, and stability. Pyrolysis behavior was analyzed using thermogravimetric analysis (TGA) and kinetic modeling (Flynn–Wall–Ozawa, Kissinger–Akahira–Sunose, and Coats-Redfern methods). Pot trials evaluated the effects of biochar on soil fertility and paddy yield. Biochar stability and carbon sequestration potential were determined using the $R_{50}$ recalcitrance index.

**Results** Among PMF, SFC, and STB biochars, PMF pyrolyzed at 500 °C (PMF500) exhibited the best characteristics, including higher nitrogen content (1.11%), a balanced C/N ratio (61.49), a high cation exchange capacity (25.29 cmol/kg), and the lowest decomposition energy threshold. These properties led to a 7.3% increase in paddy yield. PMF500 also showed moderate stability ($R_{50} = 0.53$) and a carbon sequestration potential (CSP) of 50.73%, supporting long-term carbon storage.

**Conclusion** PMF-derived biochar improves soil fertility and carbon sequestration, making it a promising soil amendment. This study advances sustainable biomass utilization and soil management, with potential applications in climate mitigation in tropical regions.

**Keywords** Palmae biomass · Biochar · Soil reclamation · Paddy pot trial · Carbon sequestration potential

Responsible editor: Hailong Wang

Kah Ho Yeong and Tao Liu equally contributed to this study.

✉ Yin Wang
yinwang@iue.ac.cn

1 State Key Laboratory of Regional and Urban Ecology, Institute of Urban Environment, Chinese Academy of Sciences, Xiamen 361021, China

2 University of Chinese Academy of Sciences, Beijing 100049, China

3 CAS Haixi Industrial Technology Innovation Center in Beilun, Ningbo 315830, China

4 Faculty of Engineering, Computing and Science, Swinburne University of Technology Sarawak Campus, 93350 Kuching, Sarawak, Malaysia

## 1 Introduction

With its tropical rainforest climate, Malaysia is rich in biomass resources and generates large quantities of Palmae biomass annually, including oil palm, sago, and coconut (Chew et al. 2023). Of these, palm oil waste accounts for more than half of Malaysia's biomass raw materials, including 6.49 million tons of palm kernel shells (PKS), 260,800 tons of empty fruit bunches (EFB), and 159,900 tons of palm mesocarp fiber (PMF) (Su et al. 2022). Besides, coconut and sago play essential roles in the Malaysian economy. The production of coconut milk generates agro by-products, such as coconut fiber (CF) and coconut shell (CS). The extraction process of sago starch also produces biomass, including sago

Published online: 09 June 2025

fiber coarse (SFC), sago fine fiber (SFF), sago trunk bark (STB), and sago trunk pith (STP) (Wan et al. 2016).

Among these biomass types mentioned above, CS, in particular, has been effectively utilized in agriculture, as a fuel, and as an adsorbent. Li et al. (2022a, b) reported that coconut shells and their biochar could effectively diminish antibiotic resistance genes (ARGs) in the soil environment. Manikandan and Nair (2023) proposed that coconut shell biochar could be used as a soil amendment to repair cadmium-contaminated soil, and the research results showed that biochar could also remove 73.84% of cadmium in soil. Moreover, coconut shell pyrolysis produces oil that can be used as a natural fuel product. Gao et al. (2016) reported a maximum oil yield of 75.74 wt% from coconut shell pyrolysis at 575 °C with a heating rate of 20 °C/min. However, other promising biomass types, such as PMF, STB, and SFC, remain underexplored in terms of their pyrolysis characteristics and soil amendment potential. PMF, STB, and SFC are often discarded or incinerated, causing environmental pollution.

Pyrolysis is a promising treatment technology that converts waste biomass into value-added products such as biochar, bio-oil, and syngas. It offers a sustainable solution to reduce environmental pollution while enhancing the utilization of renewable raw materials. Currently, coconut shells are the most studied pyrolysis material. Ashwini et al. (2024) found that the thermal degradation of coconut shells can be divided into three stages: dehydration, devolatilization, and combustion. Dehydration occurs primarily from room temperature up to about 200 °C. The devolatilization stage, occurring between 200 °C and 450 °C, is mainly attributed to the pyrolysis of cellulose and hemicellulose. After 450 °C, the coconut shell enters the carbonization stage, where the undecomposed lignin forms coconut shell carbon, which consists of fixed carbon and ash. Uddin Monir et al. (2024) conducted thermal and kinetic evaluations of coconut shells at a constant heating rate of 5 °C/min. Their analysis revealed that the Zhuravlev diffusion equation (DM6) was the most suitable model for the process, with an activation energy (Ea) of 68.9 kJ/mol. Additionally, they proposed the effects of heating rate and the model on the thermal and dynamic properties of coconut shells. Moreover, the pyrolysis temperature influences the characteristics of the coconut shell. Li et al. (2008) demonstrated that coconut shell biochar produced from high-temperature carbonization had a higher specific surface area, total volume, micropore volume, and yield compared to that obtained from low-temperature carbonization. In summary, extensive studies have examined the pyrolysis behavior of CS, focusing on the influence of pyrolysis temperature and heating rate on biochar properties, specific surface area, and stability (Dolah et al. 2021; Azman et al. 2022; Ajien et al. 2023). However, studies on PMF, SFC, and STB remain limited, with very few studies addressing their pyrolysis characteristics, thermal decomposition behavior, or kinetic parameters.

On the other hand, Malaysia's self-sufficiency rate for rice production remains around 67–70%, necessitating imports to meet domestic demand (Dorairaj and Govender 2023). This reliance on imported food underscores the urgent need to enhance local agricultural productivity. One promising strategy is integrating biochar as a soil amendment, as its ability to improve soil structure, retain moisture, and enhance nutrient availability could lead to higher crop yields and greater food security (Alkharabsheh et al. 2021; Ramamoorthy et al. 2022; Wu et al. 2022). Studies have demonstrated that biochar derived from well-studied biomass sources such as EFB, CF, and CS significantly improves soil fertility and increases crop yields (Che Ku Hafeez et al. 2020; Guarnieri et al. 2021; Bramarambika et al. 2024). One study reported that CS biochar applied at 30 t/ha improved soil pH, nutrient availability, and water retention in acidic Alfisols, leading to a 25–35% increase in the number of leaves and a 10–15% increase in fruit length, which contributed to higher yields of chili (*Capsicum annum L.*) (Bramarambika et al. 2024). Moreover, biochar produced from CS and EFB has been successfully applied to mitigate soil degradation, enhance nutrient retention, and reduce greenhouse gas emissions, further reinforcing its role in sustainable agriculture (Tisserant et al. 2023; Mishra and Mohanty 2023). Despite these promising applications, the effects of biochar derived from PMF, SFC, and STB on soil amendment, crop growth, and carbon sequestration remain largely unexplored. Understanding these underutilized biomass sources is crucial, as their biochar properties may differ significantly from those of well-studied alternatives.

In summary, biochar can enhance soil quality, improve nutrient availability, promote crop growth, and enrich soil microbial populations. Additionally, biochar contains stable carbon that can be stored in the soil (Harvey et al. 2012). When used alone, biochar increases soil organic carbon and contributes to long-term carbon sequestration, helping mitigate the effects of global warming (Xu et al. 2021). Lontsi et al. (2024) have shown that the carbon storage capacity of coconut shell and palm kernel shell biochar is 374.6 and 355.8 $CO_2$ eq $kg^{-1}$, respectively. Under the same conditions, the characteristics of biochar vary due to the differing physical and chemical properties of the original biomass. As a result, the carbon storage capacity of biochar is influenced by the type of biomass used. However, all types of biochar generally have a high carbon content, indicating significant potential for reducing $CO_2$ emissions in the atmosphere.

Therefore, this study addresses research gaps by analyzing four types of Malaysian Palmae biomass—PMF, SFC, STB, and CS—focusing on pyrolysis behavior and biochar properties. Particular attention is given to comparing the well-studied CS with the less explored PMF and SFC to systematically evaluate their physicochemical characteristics and pyrolysis kinetics at varying temperatures (300 °C, 500 °C, and 700 °C). This investigation aims to optimize pyrolysis conditions to produce high-quality biochar suitable for soil amendment applications. To assess the agricultural potential of the most promising biochar, pot experiments were conducted to evaluate its effects on soil health and crop growth. This study will contribute to advancing sustainable biomass utilization, biochar production, and agricultural soil management.

## 2 Materials and methods

### 2.1 Experimental materials

The four different Palmae biomass raw materials used in this study include palm mesocarp fiber (PMF), sago fiber coarse (SFC), sago trunk bark (STB), and coconut shell (CS). All materials were sourced from the Alliance of Bioeconomy Community Development @ Borneo, an organization based in Sabah, Malaysia. Each type was dried in an oven at 105 °C for 24 h to prepare the biomass for experimentation. Following the drying process, the materials were sealed in ziplock bags and stored in a dry location at room temperature for future use.

### 2.2 Preparation of biochar

The biomass materials were pyrolyzed in a nitrogen atmosphere using a tubular furnace, as illustrated in Fig S1. The preparation involved placing the dried samples into a quartz tube, which was then inserted into the furnace. The samples were heated at a rate of 10 °C per minute to target temperatures of 300 °C, 500 °C, and 700 °C, where they were maintained for one hour before cooling to room temperature. Once the pyrolysis was complete, the resulting biochar was ground and sieved through a 100-mesh screen to ensure uniform particle size. The prepared biochars were then sealed for subsequent characterization. Each biochar sample was labeled according to its source and pyrolysis temperature, resulting in the following designations: PMF300, PMF500, PMF700, SFC300, SFC500, SFC700, STB300, STB500, STB700, CS300, CS500, and CS700.

### 2.3 Characterization methods

The ultimate analysis of the raw materials and biochar was determined using an elemental analyzer (VARIO MAX, Germany), and oxygen content was subsequently calculated by difference (100 – [C + H + N + S + ash] %). Atomic H/C and O/C ratios were then derived from the elemental percentages using the atomic weights of H (1.008), C (12.011), and O (16.00), providing quantitative indices of aromaticity and surface polarity. Proximate analysis of raw materials and biochar, including moisture, ash, volatile matter content, and fixed carbon content, was calculated using the mass balance method by the Chinese National Standard (GB/T 28731–2012) for solid biomass fuel industrial analysis method. The specific surface area was measured by recording $N_2$ adsorption–desorption isotherms at 77 K using a pore size and surface area analyzer (SSA-7000, China). Prior to analysis, all samples were degassed under vacuum at 200 °C for 3 h to remove adsorbed moisture and volatile impurities. The measurement was performed using the Brunauer–Emmett–Teller (BET) method. Thermogravimetric analysis (TG) was performed with a Netzsch TG 209 F3 (Germany) analyzer. The procedure was carried out with temperature increasing from room temperature to 800 °C at heating rates of 10, 20, and 30 °C/min, with using approximately 10 mg of sample, under a high-purity nitrogen atmosphere and a gas flow rate set to 60 mL/min. The available phosphorus (AP) content was determined following the sodium hydrogen carbonate solution-Mo-Sb anti-spectrophotometric method, following the Chinese National Standard HJ 704–2014. Similarly, the flame photometry method determined the exchangeable potassium (AK) content, as the Chinese National Standard NY/T 889–2004 prescribed. Biochar samples'cation exchange capacity (CEC) was determined using the hexamine cobalt trichloride solution with the spectrophotometric method. At the same time, the pH measurements were conducted using an electrode method (UB-7, Denver, USA).

### 2.4 Pyrolysis kinetics analysis

The impact of pyrolysis temperature and process force on pyrolysis characteristics can be elucidated through kinetic analysis, as detailed in the Supporting Information. Several model-free methods, such as Flynn–Wall–Ozawa (FWO), Kissinger–Akahira–Sunose (KAS), and model-fitting methods like Coats-Redfern (C-R), are used to analyze the pyrolysis kinetics as shown in Table 1 (Mallick et al. 2018; Li et al. 2022b; Tariq et al. 2022). The C-R method selects the model with the highest linear fit regression coefficient $R^2$ across different temperature ranges to calculate the pyrolysis reaction parameters of the biomass. FWO and KAS methods perform calculations using the isoconversional method across multiple TG experiments. The activation energy primarily indicates the minimum energy required for reactant molecules to initiate and sustain a reaction; only molecules with kinetic energy exceeding the activation energy can overcome the energy barrier and react, while collisions between other molecules are ineffective. The activation energy is related to the reaction rate; the lower the activation energy, the faster the reaction rate.

**Table 1** Methods of thermokinetic analysis and approximate formulas

| Method | Formula | $E_a$ Calculation |
|---|---|---|
| Flynn–Wall–Ozawa (FWO) | $\ln\beta = \ln\left(\frac{AE_a}{Rg(\alpha)}\right) - 2.315 - 0.4567\frac{E_a}{RT}$ | The activation energy ($E_a$) is obtained by calculating the slope of the line formed by plotting ln(β) against (1/T) for each value of α |
| Kissinger-Akihara-Sunose (KAS) | $\ln\left(\frac{\beta}{T^2}\right) = \ln\left(\frac{AR}{E_a g(\alpha)}\right) - \frac{E_a}{RT}$ | The activation energy ($E_a$) is derived by calculating the slope of the plot between $\ln(\beta/T^2)$ and (1/T) for each value of α |
| Coats and Redfern (C-R) | $\ln\left(\frac{g(\alpha)}{T^2}\right) = \ln(\frac{AR}{\beta E_a}(1 - \frac{2RT}{E_a})) - \frac{E_a}{RT}$ | The activation energy ($E_a$) is derived by substituting a specific mechanism function into the model to analyze kinetic data |

### 2.5 Pot experiments

The pot experiment was set up using paddy soil collected from Fujian Xiang'an (24°41′ 22"N and 118°16′18"E), China, with baseline properties including pH = 5.16, CEC = 15.74 cmol/kg, and TN = 0.36%. The soil was homogenized before use to ensure consistency. Soil was filled into the jars (11 cm in height and 10.5 cm in diameter, each containing 750 g of soil). The experiment was conducted in the greenhouse of the Institute of Urban Environment, Xiamen. Three treatments were set up: (1) a control group without biochar (CK), (2) CK with a 5 wt.% PMF500 biochar, and (3) CK with a 10 wt.% PMF500 biochar, each replicated three times. Hybrid paddy seeds were planted according to the System of Rice Intensification (SRI) guidelines, using young seedlings aged eight days transplanted singly to a depth of 2 cm to preserve root integrity. A continuous flooded irrigation system was maintained throughout the growth cycle, ensuring a consistent water depth of 1–2 cm to support optimal root establishment and nutrient availability. This submerged condition is characteristic of traditional paddy field management in tropical climates, helping to sustain anaerobic soil conditions that promote rice growth and reduce methane emissions through organic matter decomposition. Water levels were lowered 7 days before harvest to facilitate grain maturation and drying. MRM-2420 infrared radiators were used to control temperature, increasing diurnal temperature by 2 °C and nocturnal temperature by 3 °C, reaching a maximum of 6 °C. Crop height was assessed at seven-day intervals throughout the growth period to observe the influence of biochar on crop growth. After 126 days, the crop was harvested, and yield was evaluated to determine the impact of various treatments on rice production. The weight of 1000-grain rice is calculated by collecting 50 grains, weighing them using a precise electronic balance, repeating the process three times for accuracy, documenting the average weight obtained, and multiplying this average by 20 to get the weight of 1000 grains.

### 2.6 Biochar stability and sequestration potential

The R50 recalcitrance index proposed by Harvey et al. (2012), along with the carbon sequestration potential (CSP) outlined by Zhao et al. (2013) was utilized to predict the stability and soil carbon sequestration of the biochar examined in this study. The $R_{50}$ recalcitrance index refers to the temperature at which 50% of the biochar undergoes oxidation or volatilization during thermal analysis. This index is determined by comparing the oxidation temperature of a specific biochar (T50, x) to that of graphite (T50, graphite), which serves as a benchmark for thermal stability. A higher $R_{50}$ value indicates greater stability and longevity in soil, enabling biochar to sequester carbon effectively over extended periods. On the other hand, CSP represents the estimated percentage of carbon that can be retained in the soil over time following biochar application. These metrics are significant as they give context to the biochar's long-term effectiveness in mitigating climate change by sequestering carbon, thereby contributing to a reduction in atmospheric $CO_2$ levels. The detailed calculations for $R_{50}$ recalcitrance, and CSP are available in Supporting Information.

## 3 Results and analysis

### 3.1 Physicochemical properties of different palmae biomass

The physicochemical properties of biomass are critical determinants of biochar quality and its subsequent effectiveness in soil amendment and carbon sequestration applications. This study compares the physicochemical characteristics of four Palmae biomass types—PMF, SFC, STB, and CS—to evaluate their suitability for biochar production. The detailed results of ultimate and proximate analyses, along with derived atomic H/C and O/C ratios are presented in Table 2.

The ultimate analysis revealed carbon (C) content across all biomass types, ranging from 40.97% to 45.48%. PMF had the lowest carbon content (40.97%), which may be attributed to its higher ash content. Sulfur (S) content was uniformly low across all samples, minimizing potential risks of soil acidification and supporting nutrient balance in amended soils (Derakhshan Nejad et al. 2021). Additionally, PMF exhibited significantly higher nitrogen (N) content (2.59%) relative to SFC (0.57%), STB (0.47%), and CS (0.23%),

**Table 2** The physicochemical properties of four biomasses

| Sample | Ultimate analysis (%) | | | | | Proximate analysis (wt %) | | | | Atomic Ratio | |
|---|---|---|---|---|---|---|---|---|---|---|---|
| | C | H | N | S | O[a] | Moisture | Ash | Volatile Matter | Fixed Carbon | H/C | O/C |
| PMF | 40.97 | 5.83 | 2.59 | 0.04 | 38.37 | 20.50 | 12.20 | 78.13 | 21.41 | 1.70 | 0.70 |
| SFC | 41.73 | 6.12 | 0.57 | 0.09 | 47.50 | 12.53 | 3.99 | 71.56 | 20.07 | 1.75 | 0.85 |
| STB | 41.60 | 6.23 | 0.47 | 0.04 | 49.24 | 11.45 | 2.42 | 75.81 | 22.21 | 1.78 | 0.89 |
| CS | 45.48 | 5,94 | 0.23 | 0.01 | 47.88 | 9.73 | 0.46 | 77.02 | 20.27 | 1.56 | 0.79 |

[*]Note: [a]O, Oxygen (by difference, O = 100 − (C + H + N + S + Ash)

suggesting enhanced potential for soil fertility improvement when converted to biochar (Ali et al. 2022).

Proximate analysis indicated notable differences in moisture and ash content among the biomass types. PMF exhibited the highest moisture content (20.50%) and ash content (12.20%), characteristics associated with increased cation exchange capacity and mineralization potential (Villegas-Pangga 2020). The relatively high ash content of PMF biomass implies significant quantities of inorganic minerals, which can contribute beneficial nutrients when applied as biochar in soils. A study by Nabila et al. (2023) indicates that ash from oil palm biomass typically contains high concentrations of potassium (K), calcium (Ca), magnesium (Mg), and other beneficial trace elements, which collectively improve soil fertility and increase soil alkalinity. However, it is essential to ensure that concentrations of potentially toxic trace elements such as cadmium (Cd), chromium (Cr), copper (Cu), nickel (Ni), and lead (Pb) are within permissible limits to minimize the risk of soil contamination (Zhang et al. 2023).

In contrast, CS displayed the lowest ash (0.46%) and sulfur content (0.01%), making it highly suitable for soil remediation applications due to minimal residual mineral interference (Zaitun et al. 2022).

Sago-derived biomass (SFC and STB) demonstrated higher volatile matter content, indicative of greater hemicellulose and cellulose concentrations. This composition enhances their reactivity during pyrolysis but may reduce the thermal stability of the resulting biochar (Nath et al. 2022). STB, with its higher fixed carbon content (22.21%), suggests a greater lignin concentration, which favors biochar stability and supports long-term carbon sequestration (Rodrigues et al. 2023).

Furthermore, the atomic H/C and O/C ratios elucidate chemical reactivity and aromatic condensation potential. PMF exhibited intermediate ratios (H/C = 1.70; O/C = 0.70), indicating a moderate degree of aromaticity with substantial oxygenated functional groups, attributes that support both microbial recalcitrance and agronomic functionality (Liew et al. 2022). The elevated oxygen (O) content in PMF reflects the presence of hydroxyl, carbonyl, and carboxylic functional groups, which facilitate nutrient retention, surface reactivity, and cation exchange mechanisms. SFC and STB exhibited higher H/C (1.75 and 1.78, respectively) and O/C ratios (0.85 and 0.89, respectively), presenting more labile, oxygen-rich constituents. These compositions may enhance reactivity and decomposability during thermochemical conversion. However, this elevated oxygen functionality simultaneously reduces chemical stability and increases susceptibility to oxidative degradation and nutrient leaching (Yuan et al. 2021). In contrast, CS demonstrated the lowest H/C ratio (1.56) and a moderately low O/C ratio (0.79), indicative of a highly condensed, lignin-rich matrix with fewer oxygen-containing functionalities, which favor long-term carbon sequestration and resistance to microbial decomposition but may limit its efficacy in agronomic applications where surface reactivity and nutrient exchange are essential (Liew et al. 2022).

The physicochemical profiles of the biomass types analyzed suggest differential suitability for specific biochar applications. PMF, with its high nitrogen content and moderate oxygen functionality, offers promising potential for soil fertility enhancement, though its higher moisture content may necessitate optimized pyrolysis conditions to ensure biochar stability. SFC and STB, enriched in hemicellulose and cellulose, demonstrate higher H/C and O/C ratios, indicative of increased reactivity but lower thermal stability and resistance to degradation. CS, characterized by low ash content and high lignin concentration, provides superior long-term carbon sequestration potential, aligning with its established use in soil remediation contexts. These findings underscore the importance of selecting appropriate biomass feedstocks based on desired biochar properties and target agricultural or environmental applications.

### 3.2 Physicochemical properties of different palmae biochar at different temperatures

The physicochemical properties of biochar pyrolyzed at various temperatures were analyzed, as indicated in Fig. 1. Since palm biomass belongs to woody biomass and consists mainly of components such as cellulose, hemicellulose, and lignin, Palmae biomass has similar characteristics in terms

**Fig. 1** Physicochemical properties of different Palmae biochar at different temperatures. (**a**) Proximate analysis (wt.%) and yield; (**b**) Specific surface area and pH

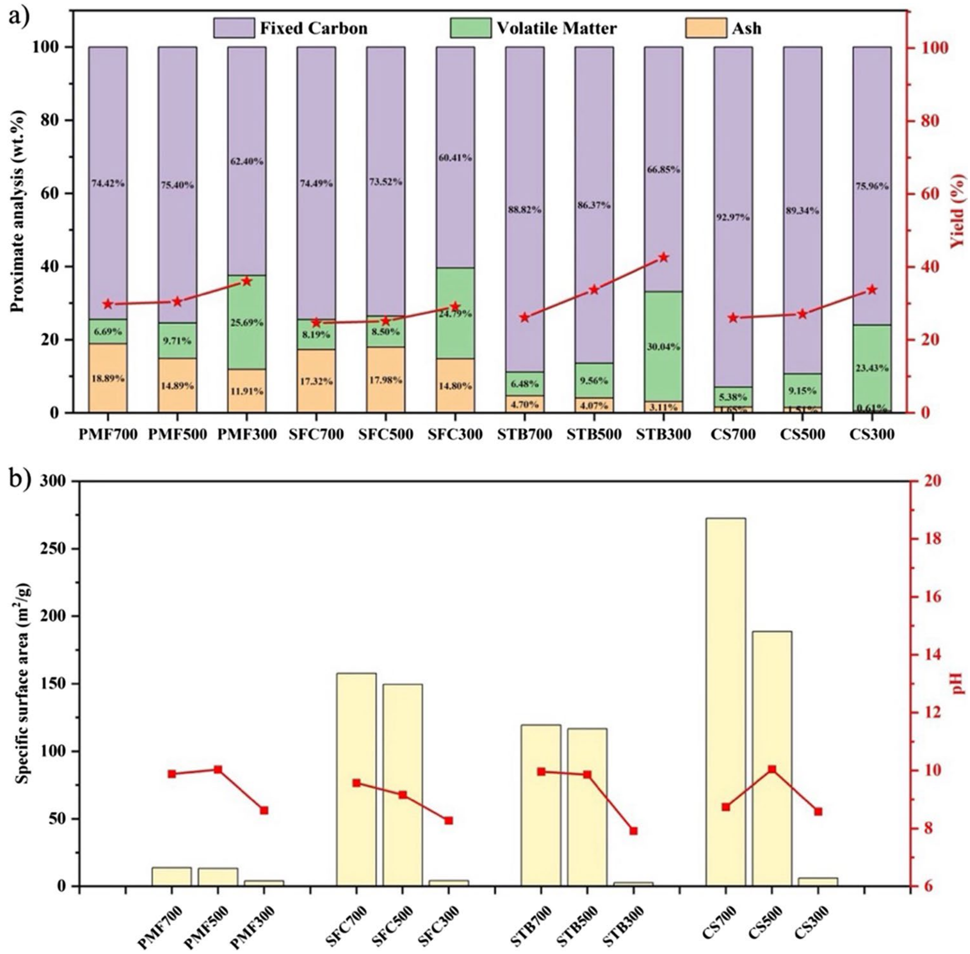


of pyrolysis yield (20 wt.% to 40 wt.%) and biochar pH (7 to 10).

In addition to the effect of the nature of the biomass itself, the pyrolysis temperature also has a crucial influence on the physicochemical properties of biochar. As indicated in Fig. 1(a), biochar yield decrease with increasing pyrolysis temperatures. The pH value of biochar produced at 300 °C is notably lower than that produced at 500 °C and 700 °C (Fig. 1(b)). However, the overall pH of biochar remains alkaline, ranging between 7 and 10, primarily due to the destruction of acidic functional groups and the formation of alkaline functional groups (Li et al. 2023). This alkalinity benefits soil remediation, as it helps neutralize acidic soils and enhances nutrient availability (Calcan et al. 2022). The higher the pH of biochar, the higher the microbial activity, which promotes the mineralization of organic matter and increases plant nutrient utilization. Additionally, this results in stronger acid neutralization capacity, further contributing to the effectiveness of biochar in improving soil conditions (Romero Millán et al. 2021).

As the pyrolysis temperature increases, the loss of organic matter leads to a corresponding increase in ash content within the biochar, enriching alkaline minerals such as potassium (K), calcium (Ca), and magnesium (Mg), further contributing to its effectiveness in improving soil fertility and structure (Reyhanitabar et al. 2020). Higher pyrolysis temperatures lead to a decrease in easily decomposable carbon compounds while increasing the proportion of stable, difficult-to-decompose carbon materials. This results in a higher fixed carbon content, which enhances the biochar's long-term carbon sequestration potential, making it a sustainable amendment for soil health (Fan et al. 2023). Generally, as pyrolysis temperatures rise, biochar yields decrease while volatile matter content diminishes (Fan et al. 2023). This characteristic is advantageous because it indicates a more stable product less likely to degrade quickly in the soil, providing more lasting benefits over time.

Notable differences exist despite the similar physicochemical properties of the biochar derived from Palmae biomass. The specific surface area of palm-derived biochar (PMF) ranges from 3.98 to 13.26 $m^2/g$, significantly lower than that of sago (SFC and STB) and coconut-derived biochar (CS). Among palm biochar, PMF700 exhibits a larger specific surface area, indicating superior adsorption capacity. Sago-derived biochar shows variation between SFC and STB. SFC biochar exhibits a larger specific surface area compared to STB biochar, indicating better adsorption capacity. Coconut-derived biochar has the highest specific surface area among the different biochar. While biochar with higher yields may have lower carbon content and specific surface area, limiting its effectiveness in enhancing soil structure and carbon sequestration (Tu et al. 2022), increased specific surface area and porosity improve soil water retention and nutrient uptake (Kalina et al. 2022). Although higher carbon content and thermal stability, typically achieved under more intense pyrolytic conditions, are beneficial for long-term soil fertility and robust carbon storage, they may also disrupt some of the microporous structures on the surface of the biochar (Ghorbani et al. 2022). Based on this analysis of physicochemical properties, a pyrolysis temperature of 500 °C is optimal. At 500 °C, the biochar balances stability, functionality, and agricultural utility. This temperature results in high fixed carbon content, suitable porosity, and a favorable pH for soil remediation. The biochar produced at this temperature demonstrates enhanced stability for long-term carbon sequestration while retaining beneficial functional groups that promote nutrient retention and microbial activity.

Consequently, PMF, SFC, and CS are recommended for further kinetic analysis as representative biomass from palm, sago, and coconut sources, respectively. STB was excluded due to its lower specific surface area, which correlates with reduced nutrient retention potential and limited effectiveness as a soil amendment. In contrast, SFC biochar exhibits a larger specific surface area, which enhances nutrient retention and water-holding capacity, making it the preferred choice for further analysis (Tomczyk et al. 2020).

### 3.3 Thermogravimetric analysis of PMF, SFC, and CS

To investigate the pyrolysis process of PMF, SFC, and CS, thermogravimetric analysis under a nitrogen atmosphere was performed; generating TG/DTG curves at different heating rates (10, 20, 30 °C/min), as shown in Fig. 2. The pyrolysis process of these three types of biomass can be broadly divided into three stages. The first stage (< 180 °C) is the moisture evaporation stage, where biomass undergoes drying and dehydration, with only water being released and a small peak appearing on the DTG curve (Mphahlele et al. 2021). The second stage (180 °C—400 °C) is the pyrolysis stage, where, as the temperature increases, the biomass rapidly decomposes, leading to a swift increase in weight loss. This is mainly due to the high-temperature decomposition of cellulose (325—375 °C) and hemicellulose (225—350 °C), with the TG curve showing a rapid decline and the DTG curve presenting the largest weight loss peak (Tauseef et al. 2022). The third stage (> 400 °C) is the carbonization stage, where the residual biomass slowly decomposes and carbonizes, primarily involving the slow carbonization of lignin (Mohd Nor Azman et al. 2023).

From the TG/DTG curves in Fig. 2, only water is released with minimal mass loss below 180 °C, indicating no pyrolysis reactions. Pyrolysis of biomass begins at 200 °C, and with increasing temperature, the rate of weight loss consistently accelerates. All three types of the biomass exhibit similar pyrolysis characteristics. Taking a heating rate of 10 °C/min as an example, after the onset of pyrolysis, the weight loss rapidly accelerates, corresponding to the DTG curve, where the maximum weight loss peak for all biomass appears in the second stage. The maximum pyrolysis rate for PMF is −6.68%/min, with a peak at 339.7 °C. The maximum pyrolysis rate for SFC is −8.67%/min, peaking at 309.1 °C. The DTG curve of CS shows two distinct peaks at 285.9 °C and 347.9 °C. The first peak at 285.9 °C (−4.51%/min) corresponds to hemicellulose and cellulose decomposition, in which hemicellulose degrades primarily between 220 °C and 315 °C, followed by cellulose breakdown from 315 °C to 400 °C (Yang et al. 2007). At higher temperatures, the second peak at 347.9 °C (−6.74%/min) corresponds to lignin depolymerization and char formation, which occurs over a broader 200–500 °C range (Apaydın Varol and Mutlu 2023). These sequential degradation events underscore the multi-component nature of CS pyrolysis and align with established thermal profiles for lignocellulosic biomass. The TG and DTG curves for all biomass examined tend to flatten around 800 °C, suggesting the main pyrolysis process is complete. SFC has the highest weight loss ratio, with a residual mass of 19.62%, lower than CS (32.73%) and PMF (20.82%). The analysis of the pyrolysis characteristics of the biomass suggests that the content of lignin or hemicellulose in CS is higher than in PMF and SFC. According to the analysis of TG/DTG curves, significant differences in total weight loss and DTG peak shapes during biomass pyrolysis are mainly related to the inherent properties of the biomass, including differences in the content of cellulose, hemicellulose, and lignin components.

Figure 2 demonstrates that the heating rate significantly influences the pyrolysis behavior of biomass, with TG/DTG curves shifting to higher temperatures as the heating rate increases. At lower heating rates, biomass particles heat more slowly, allowing for effective internal heat transfer. In contrast, rapid heating rates hinder this transfer, causing thermal lag and shifting the overall pyrolysis temperature region upward. Therefore, a moderate heating rate of around 10 °C/min is recommended to improve the analysis of weight-related quantities to temperature changes. This moderate heating rate is also crucial for optimizing the properties of biochar used in soil remediation, as it facilitates better internal heat transfer, promoting the development of a more porous structure with a higher specific surface area, which enhances the biochar's ability to adsorb contaminants and

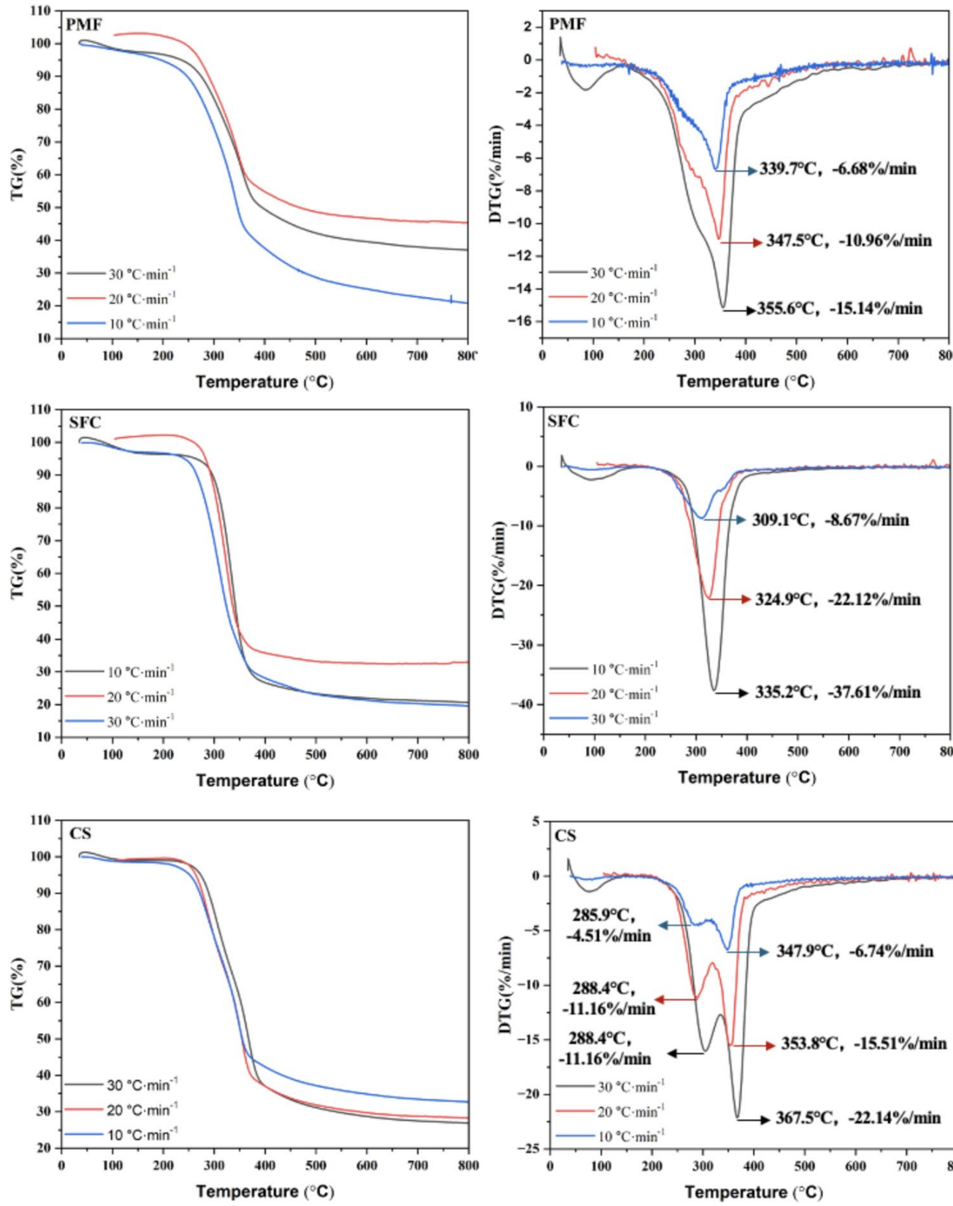


**Fig. 2** TG and DTG curves of PMF, SFC, and CS at different heating rates

retain essential functional groups that improve soil remediation potential (Mielke et al. 2023). Additionally, avoiding thermal lag ensures consistent biochar properties, such as stability and carbon content, which are key for long-term efficacy in soil improvement and pollutant sequestration (Vilas-Boas et al. 2021).

### 3.4 Pyrolysis kinetics analysis of PMF, SFC, and CS

Activation energy plays a crucial role in the ease of pyrolysis reactions, particularly in biochar production. It refers to the minimum energy required to initiate a chemical reaction and understand pyrolysis processes. Lower activation energy facilitates pyrolysis, allowing biomass to decompose at lower temperatures readily. This can lead to higher biochar yields and more efficient conversions of biomass into valuable products like bio-oil and syngas. Conversely, high activation energy requires more heat input, which can increase production costs and energy consumption. In the context of a paddy rice pot trial, biochar produced at lower temperatures tends to retain a higher concentration of micropores which can have favorable physical and chemical properties, such as enhanced porosity and subsequently better nutrient retention, which are essential for improving soil structure and water-holding capacity (Hossain et al. 2020). These properties are particularly beneficial for paddy rice cultivation, where water retention is critical (Gelardi et al. 2021). Biochar produced with lower energy input can be more cost-effective, making it a sustainable solution for large-scale agricultural practices like rice farming.

The pyrolysis kinetics of biomass are significant for its subsequent utilization and overall process optimization. Using the FWO and KAS methods for kinetic calculations of biomass pyrolysis within a temperature range of 150–800 °C and a conversion rate $\alpha$ of 0.1–0.7, step 0.1, the apparent activation energies under three heating rates (10, 20, 30 °C/min) were obtained, as depicted in Fig. 3. The fitting lines'correlation coefficients ($R^2$) for FWO and KAS methods exceed 0.90, indicating a high degree of fit.

The apparent activation energies calculated for the three types of biomass using the FWO and KAS methods show minor differences, indicating that both methods are suitable for PMF, SFC, and CS. The average activation energies for PMF, SFC, and CS obtained from the FWO and KAS methods are respectively 184.83 and 186.49 kJ/mol, 124.09 and 120.73 kJ/mol, and 158.09 and 156.46 kJ/mol. The value of E increases with the conversion rate, indicating an increase in endothermicity as biomass conversion progresses (Karuppasamy Vikraman et al. 2021). As the conversion rate $\alpha$ increases from 0.1 to 0.7, the E values of all three biomass types show a generally increasing trend, suggesting that as temperature rises, the decomposition of hard-to-degrade organic substances gradually begins, hence the continuous increase in activation energy and the reaction difficulty with the degree of reaction. Fluctuations in E values at different conversion rates indicate that the pyrolysis reaction process is not a single reaction mechanism.

As shown in Table 3, when analyzing the pyrolysis process of the three types of biomass using the C-R method with a reaction order n = 1, correlation coefficients for the fitting curves of PMF, SFC, and CS at heating rates of 10,

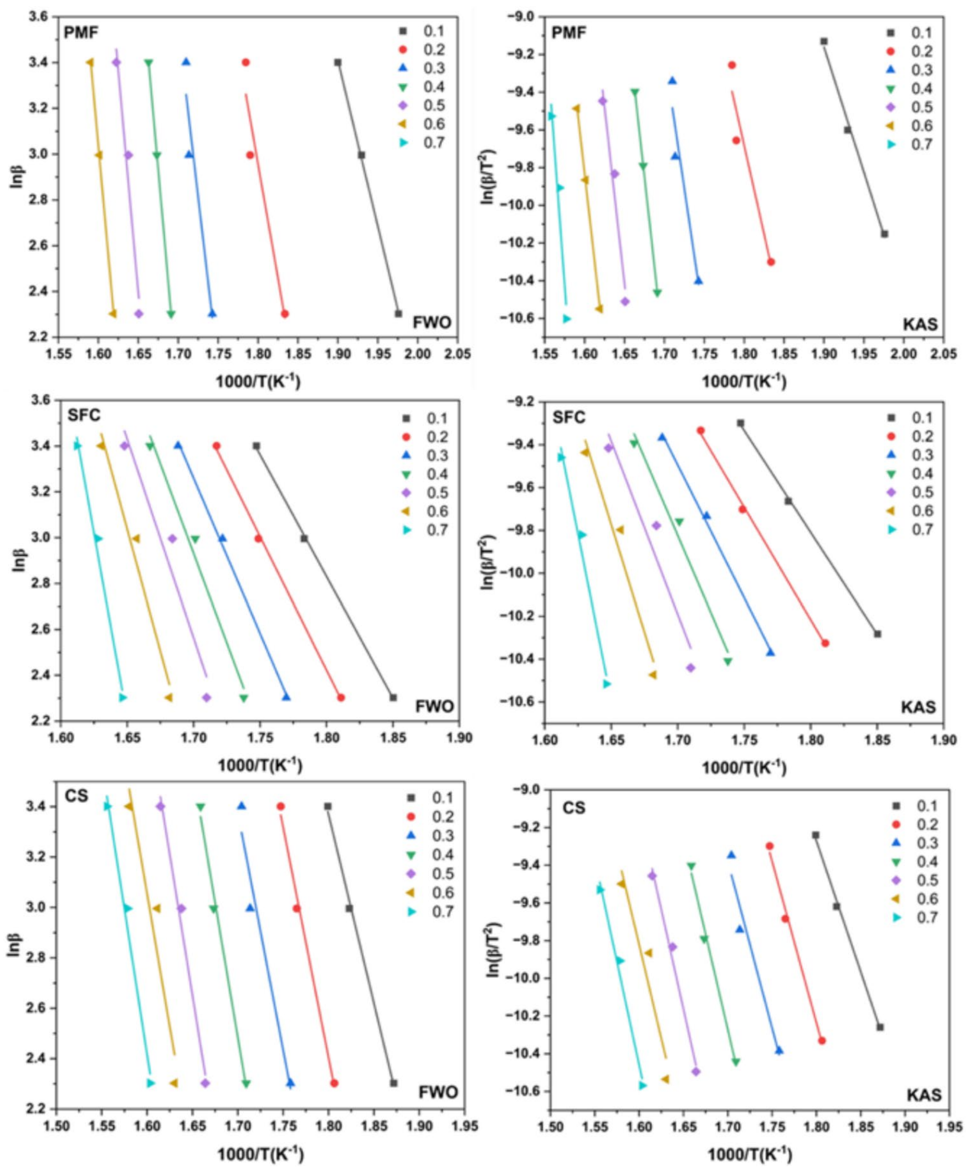


**Fig. 3** Kinetic diagrams of PMF, SFC, CS based on FWO and KAS methods

20, and 30 °C/min all exceed 0.98, demonstrating that the kinetic equations derived from n = 1 can accurately simulate the biomass pyrolysis process. The activation energy calculated for CS remains relatively stable across different heating rates, suggesting that the heating rate has a minor impact on the CS pyrolysis activation energy obtained via the C-R method. In contrast, the activation energies calculated for PMF and SFC show significant variation with heating rates, indicating a more considerable effect of heating rate on the pyrolysis activation energy for PMF and SFC, with the highest activation energy at a heating rate of 20 °C/min. The average activation energies calculated using the C-R method for PMF, SFC, and CS are 60.71, 112.01, and 67.03 kJ/mol, respectively. The C-R method views the pyrolysis process as a single reaction, thus resulting in lower activation energies than the FWO and KAS methods. The pre-exponential factor A value indicates the complexity of the pyrolysis reaction, with higher values representing more complex reactions and lower values indicating surface reactions (Merdun and Laougé 2021). Among the three biomass types studied, SFC exhibits the highest activation energy, followed by CS and PMF. This suggests that SFC requires a higher initial pyrolysis temperature and consumes more external energy than CS and PMF. Table 3 showed activation energies of biomass pyrolysis at different heating rates determined by the Coats-Redfern (C-R) method.

The analysis of pyrolysis kinetics highlights distinct energy requirements for decomposition among the biomasses. SFC demands the most energy input, making its pyrolysis process less efficient, whereas PMF exhibits the lowest energy threshold, favoring cost-effective conversion at lower temperatures. CS demonstrates stable decomposition across varying heating rates, ensuring reliability in pyrolysis applications. Despite these variations, all three biomasses exhibit a progressive increase in activation energy with conversion rate, indicating analogous degradation pathways in advanced pyrolysis stages. These insights affirm the viability of PMF and SFC as complementary biochar sources alongside CS, with each biomass offering unique advantages for targeted agricultural and environmental uses.

### 3.5 Preferred biochar for soil amendment

Evaluating the physicochemical properties of biochar is essential to determine its effectiveness as a soil amendment. Key indicators include pH, CEC, C/N ratio, and specific surface area (SSA), all of which influence nutrient retention, soil fertility, and crop productivity (Table 4).

As shown in Table 4, PMF500, SFC500, and CS500 are all alkaline with pH values greater than 9. The higher the pH of biochar, the higher the microbial activity, the higher the mineralization of organic matter, the higher the plant nutrient utilization, and the stronger the acid neutralization due to the dissolution of basic oxides and carbonates formed during pyrolysis, which react with acidic components in the soil to neutralize pH (Romero Millán et al. 2021).

PMF500 has the highest CEC value, followed by CS500 and SFC500. While the CEC value of PMF500, which is 25.29 cmol/kg is substantial for biochar, it remains lower than soil organic matter, which typically exhibits CEC values of around 200 cmol/kg or higher. This underscores biochar's relative contribution, which enhances soil properties primarily through nutrient retention, reduction in leaching, and facilitation of microbial activity rather than solely relying on CEC. Biochar with high CEC can maximize plant nutrient uptake, improve root development and soil fertility, and thus maximize crop yields (Hansen et al. 2016).

Furthermore, an appropriate C/N ratio in biochar is important for effectively enhancing soil fertility and

**Table 3** Activation energies of biomass pyrolysis at different heating rates determined by the Coats-Redfern (C-R) method

| β/ °C/min | PMF | | SFC | | CS | |
|---|---|---|---|---|---|---|
| | E/ kJ/mol | $R^2$ | E/ kJ/mol | $R^2$ | E/ kJ/mol | $R^2$ |
| 10 | 52.02 | 0.99 | 80.10 | 0.99 | 62.01 | 0.99 |
| 20 | 71.19 | 0.99 | 139.48 | 0.99 | 71.19 | 0.99 |
| 30 | 58.91 | 0.99 | 116.45 | 0.99 | 67.88 | 0.98 |
| Average | 60.71 | - | 112.01 | - | 67.03 | - |

**Table 4** Physicochemical properties of PMF500, SFC500 and CS500

| Sample | pH | CEC/ cmol/kg | C/% | N/% | C/N | SSA/ $m^2$/g |
|---|---|---|---|---|---|---|
| PMF500 | 10.03 | 25.29 | 68.25 | 1.11 | 61.49 | 13.26 |
| SFC500 | 9.16 | 8.01 | 69.19 | 0.11 | 629.00 | 149.54 |
| CS500 | 10.04 | 10.01 | 70.70 | 0.06 | 1178.33 | 188.68 |

supporting crop growth (Phillips et al. 2022). High carbon content in biochar typically increases the C/N ratio, impacting soil microbial function and reducing crop-available nitrogen (Xu et al. 2022). PMF500, with high carbon content (68.25%) and balanced C/N ratio (61.49), makes it suitable for improving soil organic matter and providing a slow release of nitrogen for crop growth. In contrast, SFC500 and CS500 exhibit extremely high C/N ratios (629.00 and 1178.33, respectively), may immobilize soil nitrogen, and thus limit crop growth unless additional nitrogen is supplied. While CS500 (188.68 $m^2/g$) and SFC500 (149.54 $m^2/g$) display higher specific surface areas compared to PMF500 (13.26 $m^2/g$), high specific surface area alone does not guarantee agronomic benefit. Greater specific surface area enhances water and nutrient adsorption via increased microporosity, but it often comes at the expense of functional exchange sites (–COOH, –OH) and nutrient content lost at higher pyrolysis temperatures (Maziarka et al. 2021). PMF500 instead combines sufficient microporosity with abundant exchange sites (high CEC) and essential nutrients (N and ash-derived $K^+$, $Ca^{2+}$, $Mg^{2+}$), yielding superior crop performance.

Antonangelo et al. (2024) emphasize that CEC and nutrient balance, particularly nitrogen content, are more reliable predictors of biochar performance in improving soil fertility and crop productivity than specific surface area alone. While a larger specific surface area enhances the adsorption of nutrients and water, its direct influence on plant nutrient uptake and soil health is secondary. The higher nitrogen content in PMF500 (1.11%) facilitates gradual nutrient release, supporting sustained crop growth and promoting long-term soil fertility. Therefore, the synergy of alkalinity, balanced C/N, high CEC, and inherent nutrient supply of PMF500 underlies its optimal performance as a soil amendment and explains its agronomic superiority over biochars with higher specific surface area but fewer exchange sites.

While there is a wealth of current research on the use of CS for soil amendment, studies on PMF remain scarce. Given the growing interest in sustainable agricultural practices and the potential advantages of utilizing diverse biomass sources, investigating PMF as a soil amendment is both timely and essential. By selecting PMF500 for this study, we aim to address this critical gap in the literature, offering valuable insights into its effects on soil properties and crop growth while expanding the range of biomass resources available for soil enhancement. Therefore, PMF500 was selected to verify its effect on soil properties and crop growth.

### 3.6 Efficacy of PMF500 biochar in soil properties and crop growth

To explore the impact of adding PMF500 biochar on soil nutrients, the changes in soil CEC, pH, TN, AP, and AK pre- and post-treatment were examined (Fig. 4). Figure 4(a) illustrates that adding PMF500 biochar significantly enhanced the soil CEC. The CK + 10% Biochar treatment achieved a CEC of 18.35 cmol/kg, and CK + 5% Biochar reached 17.43 cmol/kg, both markedly higher than the CK (15.74 cmol/kg). This increase can be attributed to the high specific surface area and porous structure of the biochar, which improve the soil's ability to retain nutrients such as potassium ($K^+$), ammonium ($NH_4^+$), calcium ($Ca^{2+}$), and magnesium ($Mg^{2+}$) (Haque et al. 2021). Simultaneously, it reduced nutrient leaching and increased nutrient availability for crop uptake. Furthermore, biochar treatments significantly increased soil pH. The CK + 10% PMF500 treatment raised the pH to 5.37, while the CK + 5% PMF500 treatment resulted in a pH of 5.47, compared to the control group (CK), which had a pH of 5.16. The alkaline nature of biochar, attributed to the presence of basic oxides and carbonates formed during pyrolysis, helps neutralize soil acidity. This process involves

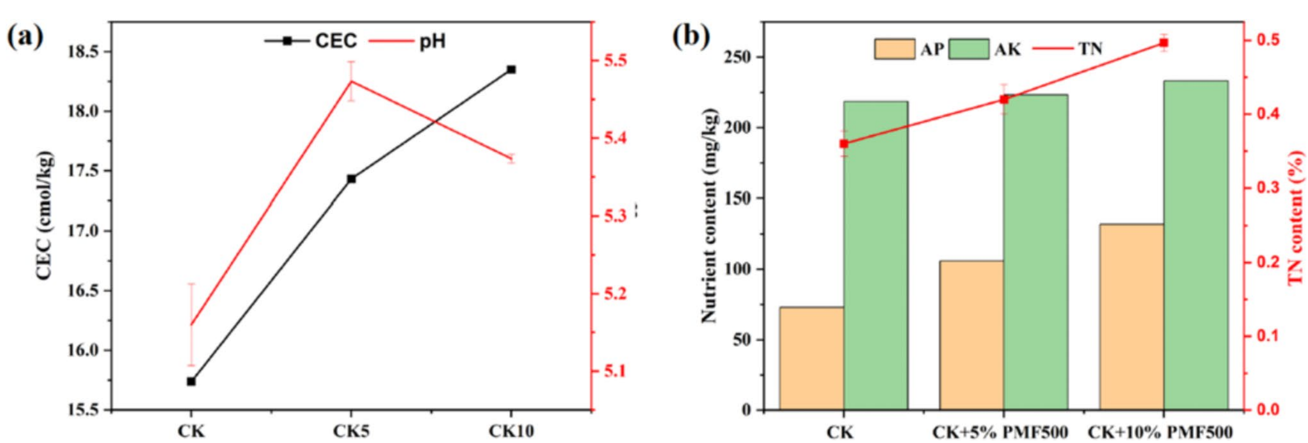


Fig. 4 Soil properties of three control groups. **a** CEC contents and pH, and (**b**) TN, AP, and AK contents

the dissolution of the basic compounds, which react with the acidic components in the soil, ultimately leading to an increase in soil pH (Shen and Yuan 2021).

The TN, AP, and AK content were notably higher in the PMF500 biochar-treated soils, as shown in Fig. 4(b). The TN content of CK + 10% PMF500 was 0.49%, and that of CK + 5% PMF500 was 0.42%, which was higher than those of the CK (0.36%). The porous structure of biochar facilitates nitrogen adsorption, reduces nitrogen leaching, and provides a slow release of nitrogen, thereby improving nitrogen use efficiency (Jia et al. 2021). The CK + 10% PMF500 treatment had an AP of 132 mg/kg, and CK + 5% PMF500 showed 106 mg/kg, compared to the CK (73 mg/kg). This increase may be attributed to biochar's high specific surface area, which can potentially adsorb phosphate ions, reducing their leaching and enhancing crop availability. CK + 10% PMF500 resulted in an AK value of 233 mg/kg, and CK + 5% PMF500 showed 223 mg/kg, both higher than CK (218 mg/kg). Biochar helps retain potassium in the soil, reducing its leaching and enhancing crop availability (Lv et al. 2021). The addition of PMF500 biochar significantly improves soil properties, with the CK + 10% PMF500 treatment exhibiting the most substantial improvements across all evaluated parameters.

To investigate the impact of adding PMF500 on crop growth, variations in crop height and rice yield after the application of PMF500 biochar were examined (Fig. 5). As illustrated in Fig. 5(a), the crop height of CK + 10% PMF500 and CK + 5% PMF500 treatments was higher than that of CK. For instance, on day 28, the average CK + 10% PMF500 height was 14.23 cm, CK + 5% biochar was 14.08 cm, and CK was 11.86 cm. The yield of rice also confirmed the effect of biochar on crop growth. The 1000-grain weight serves not only as an indicator of grain quality but also provides a reliable estimate of rice yield. Figure 5(b) investigates the effects of PMF500 on the 1000-grain weight of rice and the rice yield at harvest, demonstrating notable improvements in rice quality and potential yield. The control group, CK, showed an average 1000-grain weight of 14.47 g.

Specifically, CK + 5% PMF500 treatments resulted in an average 1000-grain weight of 15.93 g, while the CK + 10% PMF500 treatments further increased this metric to 18.41 g. These enhancements are likely due to biochar's ability to improve soil structure, enhance nutrient retention and availability, and boost microbial activity (Cacal et al. 2023). Higher 1000-grain weights indicate improved grain quality, as heavier grains tend to be plumper and better filled, resulting from optimal nutrient uptake and favorable growing conditions. Besides that, as illustrated in Fig. 5(b), the yield of rice from CK + 10% PMF500 was 7.21% higher than that of CK. The difference in yield between CK + 10% PMF500 and CK indicated that biochar's high specific surface area and porosity could improve soil properties and nutrient availability and promote the adsorption and retention of nutrients in the soil matrix, making them more available to crops. This is consistent with the findings from Biederman and Harpole (Biederman and Harpole 2013), which suggested that biochar application could enhance nutrient retention in soil and increase nutrient availability. They observed a proportional relationship between increased 1000-grain weight and rice yield, suggesting that biochar enhances grain quality and contributes to higher yields. This finding is consistent with recent research by Cacal et al. (2023), which reported similar benefits of biochar in improving grain weight and yield in rice cultivation. Therefore, adding PMF500 biochar significantly enhanced rice quality and yield.

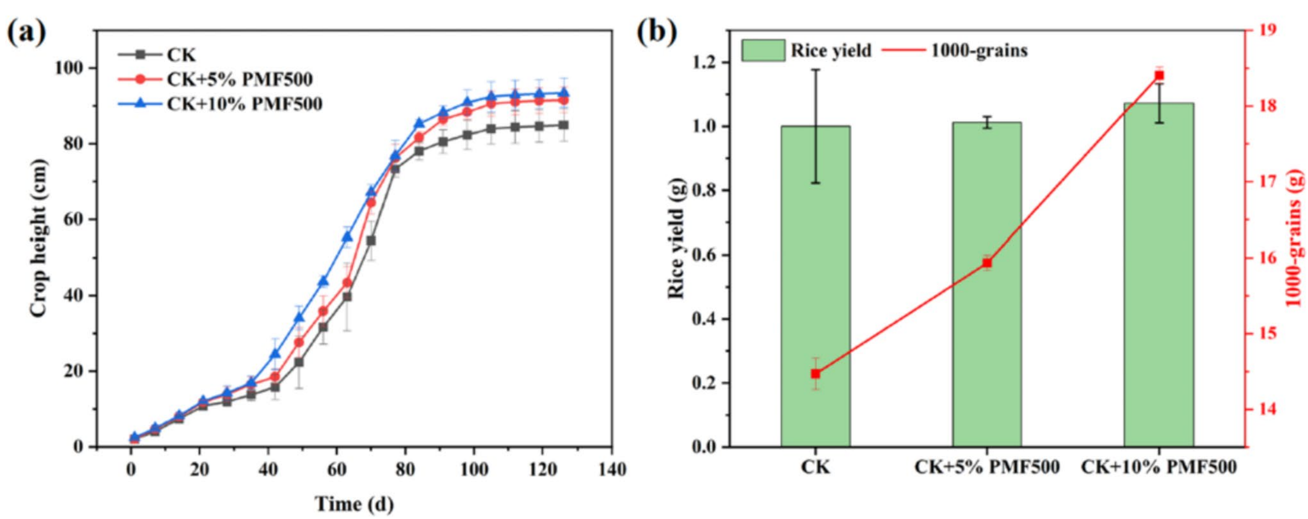


**Fig. 5** **a** crop height of different treatments, **b** rice yield, and 1000 grains of various treatments

### 3.7 Biochar stability and sequestration potential

The longevity and stability of biochar carbon are influenced by its physicochemical properties, interactions with soil, and environmental conditions. Evaluating the recalcitrance index ($R_{50}$) and carbon sequestration potential (CSP) is essential for assessing biochar suitability for long-term carbon storage and climate mitigation. Based on $R_{50}$ classification, biochars are categorized as highly resistant ($R_{50} \geq 0.7$), moderately resistant ($0.5 \leq R_{50} < 0.7$), or degradable ($R_{50} < 0.5$). In this study, PMF500 biochar was evaluated for its stability and sequestration potential, yielding an $R_{50}$ value of 0.53, indicating moderate resistance to degradation. This suggests that PMF500 biochar has long-term sequestration potential, particularly due to its high fixed carbon content (68.25%) and cation exchange capacity (CEC = 25.29 cmol/kg), which supports stable interactions with soil components. The estimated CSP for PMF500 biochar was 50.73%, indicating its significant role in carbon retention (Table S3, Supporting Information).

To estimate the carbon sequestration impact, three utilization scenarios were considered (Table 5). Under Scenario A (100% utilization of available residues), 2.16 Mt/year of PMF biochar could be produced, sequestering 1.47 Mt of carbon, equivalent to 5.39 Mt of $CO_2$/year. In reduced availability scenarios, the sequestration potential decreases proportionally, with Scenario B (50% utilization) sequestering 2.70 Mt of $CO_2$/year and Scenario C (10% utilization) storing 0.54 Mt of $CO_2$/year. Although some biochar carbon will gradually degrade, the long-term carbon storage potential remains significant, estimated at 4.33 Mt of $CO_2$/year in Scenario A, 2.17 Mt in Scenario B, and 0.43 Mt in Scenario C. While the sequestration impact of PMF500 biochar is modest at the global scale, it represents a significant localized benefit for carbon mitigation, sustainable waste management, and soil fertility enhancement, particularly in biomass-rich regions like Malaysia.

However, $R_{50}$ reflects only laboratory-based thermal recalcitrance and may overestimate biochar persistence under real soil conditions, where microbial decomposition and physicochemical weathering at ambient temperatures significantly alter biochar structure and carbon release (Wang et al. 2020). To address these limitations, future work should include long-term laboratory and field biodegradation assays (such as soil incubation with $CO_2$ flux monitoring) and advanced structural characterization through solid-state $^{13}C$ NMR spectroscopy to track molecular transformations in situ.

In conclusion, PMF500 biochar exhibits moderate stability ($R_{50} = 0.53$) and a significant carbon sequestration potential of up to 5.39 Mt $CO_2$/year under full utilization. While its stability requires optimization, it offers a balance between soil fertility enhancement and carbon storage. To maximize long-term sequestration potential, post-pyrolysis modifications and biochar blending strategies should be explored. Future field trials are necessary to optimize its practical applicability in sustainable agriculture and climate mitigation efforts.

## 4 Conclusion

This study investigated in detail the pyrolysis characteristics of PMF, SFC, and STB, as well as their potential as soil amendments and for carbon sequestration, with CS—widely studied in previous research—used for comparative analysis. The pyrolysis characteristics of palm biomass are similar and can be divided into three stages: dehydration (< 200 °C), devolatilization (200–400 °C), and carbonization (> 400 °C). The results showed that as the heating rate increased, the weight loss rate accelerated significantly, while the activation energy slightly decreased. As pyrolysis temperature increases, ash and fixed-carbon contents increase, while volatile matter and overall biochar yield decrease; conversely, both the specific surface area and pH of the biochar increase. Among the analyzed biochars, PMF biochar pyrolyzed at 500 °C with a heating rate of 10 °C/min exhibited superior properties, including a carbon-to-nitrogen ratio of 61.49 and a cation exchange capacity of 25.29 cmol/kg, indicating a strong soil fertility potential. The pot trials demonstrated

**Table 5** Summary of the theoretical potential for PMF500 biochar production and long-term carbon storage across different utilization scenarios (A, B, and C)

| | Scenario A | Scenario B | Scenario C |
|---|---|---|---|
| Biomass Availability (Mt/year) | 7.10 (Aljuboori 2013) | 3.55 | 0.71 |
| Pyrolysis Yield (%wt.) | 30.45 | 30.45 | 30.45 |
| Biochar Yield (Mt/year) | 2.16 | 1.08 | 0.22 |
| Biochar Carbon (Mt/year) | 1.47 | 0.74 | 0.15 |
| $CO_{2eq}$ of Biochar Carbon (Mt/year) | 5.39 | 2.7 | 0.54 |
| C Remaining Long-Term (Mt/year) | 1.18 | 0.59 | 0.12 |
| $CO_{2eq}$ of C Stored Long-Term (Mt/year) | 4.33 | 2.17 | 0.43 |

*Note: Scenario A assumes 100% of residues are utilized, Scenario B represents 50% of residues availability, while Scenario C adopts a 10% availability of residues a 7.3% increase in paddy yield, while PMF500's moderate stability ($R_{50}$ = 0.53) and CSP (50.73%) support long-term carbon retention. Scenario-based estimations indicate PMF500 biochar could sequester up to 5.39 Mt $CO_2$ annually under full biomass utilization. PMF500 biochar provides localized benefits for carbon storage, soil improvement, and sustainable waste management. The combination of yield improvement, stability, and nutrient retention makes PMF500 an effective soil amendment. This study provides valuable insights into optimizing biochar production from underutilized Palmae biomass, promoting sustainable agriculture and improving soil management in tropical regions.

**Supplementary Information** The online version contains supplementary material available at https://doi.org/10.1007/s11368-025-04046-2.

**Acknowledgements** This work was funded by the ANSO Collaborative Research Project [Grant No. ANSO-CR-KP-2021-08], the STS Plan Supporting Projects of the Chinese Academy of Sciences in Fujian Province [Grant No.: 2023 T3032, and 2023 T3073] and the Alliance of National and International Science Organizations for the Belt and Road Regions [Grant No. ANSO-PA-2023-18].

**Author contributions** Kah Ho Yeong and Tao Liu conducted the experiments, and wrote the original draft of the manuscript, while Lee Tung Tan and Jiuan Jing Chew reviewed, edited, and visualized the manuscript. Yin Wang was responsible for conceptualization, validation, writing, reviewing, and editing, as well as supervision.

**Data availability** The data used to support the findings of this study are available from the corresponding author upon request.

## Declarations

**Ethical approval** Not applicable.

**Consent to participate** Not applicable.

**Consent to publish** Not applicable.

**Competing interests** The authors declare that they have no known competing financial interests or personal relationships that could have appeared to influence the work reported in this paper.

## References

Ajien A, Idris J, Md Sofwan N et al (2023) Coconut shell and husk biochar: a review of production and activation technology, economic, financial aspect and application. Waste Manag Res J Sustain Circ Econ 41:37–51. https://doi.org/10.1177/0734242X221127167

Ali I, Adnan M, Ullah S et al (2022) Biochar combined with nitrogen fertilizer: a practical approach for increasing the biomass digestibility and yield of rice and promoting food and energy security. Biofuels Bioprod Biorefining 16:1304–1318. https://doi.org/10.1002/bbb.2334

Aljuboori AHR (2013) Oil palm biomass residue in Malaysia : availability and sustaunability. IJBR 2:13. https://doi.org/10.61762/ijbrvol2iss1art13850

Alkharabsheh HM, Seleiman MF, Battaglia ML et al (2021) Biochar and its broad impacts in soil quality and fertility, nutrient leaching and crop productivity: a review. Agronomy 11:993. https://doi.org/10.3390/agronomy11050993

Antonangelo JA, Culman S, Zhang H (2024) Comparative analysis and prediction of cation exchange capacity via summation: influence of biochar type and nutrient ratios. Front Soil Sci 4:1371777. https://doi.org/10.3389/fsoil.2024.1371777

ApaydınVarol E, Mutlu Ü (2023) TGA-FTIR analysis of biomass samples based on the thermal decomposition behavior of hemicellulose, cellulose, and lignin. Energies 16:3674. https://doi.org/10.3390/en16093674

Ashwini K, Resmi R, Reghu R (2024) Pyrolysis characteristics and kinetic analysis of coconut shell and nutmeg shell for potential source of bioenergy. Eng Sci Technol Int J 50:101615. https://doi.org/10.1016/j.jestch.2024.101615

Azman NA, Asmadi M, Nawawi MAS et al (2022) Optimization of biochar production from slow pyrolysis of oil palm waste. Chem Eng Trans 97:163–168. https://doi.org/10.3303/CET2297028

Biederman LA, Harpole WS (2013) Biochar and its effects on plant productivity and nutrient cycling: a meta-analysis. GCB Bioenergy 5:202–214. https://doi.org/10.1111/gcbb.12037

Bramarambika S, Mamatha B, Jakir Hussain KN et al (2024) The effect of coconut shell biochar on the growth and yield of chilli (Capsicum annum L.) in acidic alfisols soil. J Adv Biol Biotechnol 27:203–211. https://doi.org/10.9734/jabb/2024/v27i7980

Cacal DM, Santos AR, Hipolito MC, Morales SRF (2023) Productivity of inbred rice applied with biochar under different planting distances. Asian J Agric Rural Dev 13:192–205. https://doi.org/10.55493/5005.v13i3.4829

Calcan SI, Pârvulescu OC, Ion VA et al (2022) Effects of biochar on soil properties and tomato growth. Agronomy 12:1824. https://doi.org/10.3390/agronomy12081824

Che Ku Hafeez CKD, Daljit Singh KS, Arifin A, Keeren SR (2020) Effects of Empty Fruit Bunch (EFB) application on oil palm yield, soil properties and cost-benefits analysis. J Environ Sci Pollut Res 6:435–437. https://doi.org/10.30799/jespr.208.20060301

Chew TW, H'Ng PS, Luqman Chuah Abdullah BCTG et al (2023) A review of bio-based activated carbon properties produced from different activating chemicals during chemicals activation process on biomass and its potential for Malaysia. Materials 16:7365. https://doi.org/10.3390/ma16237365

Derakhshan Nejad Z, Rezania S, Jung MC et al (2021) Effects of fine fractions of soil organic, semi-organic, and inorganic amendments on the mitigation of heavy metal(loid)s leaching and bioavailability in a post-mining area. Chemosphere 271:129538. https://doi.org/10.1016/j.chemosphere.2021.129538

Dolah R, Karnik R, Hamdan H (2021) A Comprehensive review on biofuels from oil palm empty bunch (EFB): current status, potential, barriers and way forward. Sustainability 13:10210. https://doi.org/10.3390/su131810210

Dorairaj D, Govender NT (2023) Rice and paddy industry in Malaysia: governance and policies, research trends, technology adoption and resilience. Front Sustain Food Syst 7:1093605. https://doi.org/10.3389/fsufs.2023.1093605

Fan J, Duan T, Zou L, Sun J (2023) Characteristics of dissolved organic matter composition in biochar: effects of feedstocks and pyrolysis temperatures. Environ Sci Pollut Res 30:85139–85153. https://doi.org/10.1007/s11356-023-28431-x

Gao Y, Yang Y, Qin Z, Sun Y (2016) Factors affecting the yield of bio-oil from the pyrolysis of coconut shell. Springerplus 5:333. https://doi.org/10.1186/s40064-016-1974-2

Gelardi DL, Ainuddin I, Rippner DA et al (2021) Biochar alters hydraulic conductivity and inhibits nutrient leaching in two agricultural soils. Soil 7:811–825. https://doi.org/10.5194/soil-7-811-2021

Ghorbani M, Amirahmadi E, Neugschwandtner RW et al (2022) The impact of pyrolysis temperature on biochar properties and its effects on soil hydrological properties. Sustainability 14:14722. https://doi.org/10.3390/su142214722

Guarnieri SF, Nascimento ECD, Costa Junior RF et al (2021) Coconut fiber biochar alters physical and chemical properties in sandy soils. Acta Sci Agron 43:e51801. https://doi.org/10.4025/actasciagron.v43i1.51801

Hansen V, Hauggaard-Nielsen H, Petersen CT et al (2016) Effects of gasification biochar on plant-available water capacity and plant growth in two contrasting soil types. Soil Tillage Res 161:1–9. https://doi.org/10.1016/j.still.2016.03.002

Haque ANA, Uddin MdK, Sulaiman MF et al (2021) Biochar with alternate wetting and drying irrigation: a potential technique for paddy soil management. Agriculture 11:367. https://doi.org/10.3390/agriculture11040367

Harvey OR, Kuo L-J, Zimmerman AR et al (2012) An Index-based approach to assessing recalcitrance and soil carbon sequestration potential of engineered black carbons (Biochars). Environ Sci Technol 46:1415–1421. https://doi.org/10.1021/es2040398

Hossain MZ, Bahar MM, Sarkar B et al (2020) Biochar and its importance on nutrient dynamics in soil and plant. Biochar 2:379–420. https://doi.org/10.1007/s42773-020-00065-z

Jia Y, Hu Z, Ba Y, Qi W (2021) Application of biochar-coated urea controlled loss of fertilizer nitrogen and increased nitrogen use efficiency. Chem Biol Technol Agric 8:3. https://doi.org/10.1186/s40538-020-00205-4

Kalina M, Sovova S, Svec J et al (2022) The effect of pyrolysis temperature and the source biomass on the properties of biochar produced for the agronomical applications as the soil conditioner. Materials 15:8855. https://doi.org/10.3390/ma15248855

Karuppasamy Vikraman V, Praveen Kumar D, Boopathi G, Subramanian P (2021) Kinetic and thermodynamic study of finger millet straw pyrolysis through thermogravimetric analysis. Bioresour Technol 342:125992. https://doi.org/10.1016/j.biortech.2021.125992

Li W, Yang K, Peng J et al (2008) Effects of carbonization temperatures on characteristics of porosity in coconut shell chars and activated carbons derived from carbonized coconut shell chars. Ind Crops Prod 28:190–198. https://doi.org/10.1016/j.indcrop.2008.02.012

Li H, Wang X, Tan L et al (2022a) Coconut shell and its biochar as fertilizer amendment applied with organic fertilizer: efficacy and course of actions on eliminating antibiotic resistance genes in agricultural soil. J Hazard Mater 437:129322. https://doi.org/10.1016/j.jhazmat.2022.129322

Li Y, Zhao H, Sui X et al (2022b) Studies on individual pyrolysis and co-pyrolysis of peat–biomass blends: thermal decomposition behavior, possible synergism, product characteristic evaluations and kinetics. Fuel 310:122280. https://doi.org/10.1016/j.fuel.2021.122280

Li L, Long A, Fossum B, Kaiser M (2023) Effects of pyrolysis temperature and feedstock type on biochar characteristics pertinent to soil carbon and soil health: a meta-analysis. Soil Use Manag 39:43–52. https://doi.org/10.1111/sum.12848

Liew YW, Arumugasamy SK, Selvarajoo A (2022) Potential of biochar as soil amendment: prediction of elemental ratios from pyrolysis of agriculture biomass using artificial neural network. Water Air Soil Pollut 233:54. https://doi.org/10.1007/s11270-022-05510-2

Lontsi GRM, Djousse BMK, Pernot C, Munson AD (2024) Production and characterization of eight biochars originating from agricultural waste in Cameroon. J Mater Cycles Waste Manag 26:3280–3290. https://doi.org/10.1007/s10163-024-02022-5

Lv R, Wang Y, Yang X et al (2021) Adsorption and leaching characteristics of ammonium and nitrate from paddy soil as affected by biochar amendment. Plant Soil Environ 67:8–17. https://doi.org/10.17221/276/2020-PSE

Mallick D, Poddar MK, Mahanta P, Moholkar VS (2018) Discernment of synergism in pyrolysis of biomass blends using thermogravimetric analysis. Bioresour Technol 261:294–305. https://doi.org/10.1016/j.biortech.2018.04.011

Manikandan SK, Nair V (2023) Dual-role of coconut shell biochar as a soil enhancer and catalyst support in bioremediation. Biomass Convers Biorefin. https://doi.org/10.1007/s13399-023-04079-y

Maziarka P, Sommersacher P, Wang X et al (2021) Tailoring of the pore structures of wood pyrolysis chars for potential use in energy storage applications. Appl Energy 286:116431. https://doi.org/10.1016/j.apenergy.2020.116431

Merdun H, Laougé ZB (2021) Kinetic and thermodynamic analyses during co-pyrolysis of greenhouse wastes and coal by TGA. Renew Energy 163:453–464. https://doi.org/10.1016/j.renene.2020.08.120

Mielke KC, Brochado MGDS, Laube AFS et al (2023) Pyrolysis temperature vs. application rate of biochar amendments: impacts on soil microbiota and metribuzin degradation. Int J Mol Sci 24:11154. https://doi.org/10.3390/ijms241311154

Mishra RK, Mohanty K (2023) A review of the next-generation biochar production from waste biomass for material applications. Sci Total Environ 904:167171. https://doi.org/10.1016/j.scitotenv.2023.167171

Mohd Nor Azman NAN, Asmadi M, Amin NAS et al (2023) Polycyclic aromatic hydrocarbons occurrences in biomass char and its mitigation approaches: a mini review. ChemBioEng Rev 10:462–479. https://doi.org/10.1002/cben.202200031

Mphahlele K, Matjie RH, Osifo PO (2021) Thermodynamics, kinetics and thermal decomposition characteristics of sewage sludge during slow pyrolysis. J Environ Manage 284:112006. https://doi.org/10.1016/j.jenvman.2021.112006

Nabila R, Hidayat W, Haryanto A et al (2023) Oil palm biomass in Indonesia: Thermochemical upgrading and its utilization. Renew Sustain Energy Rev 176:113193. https://doi.org/10.1016/j.rser.2023.113193

Nath H, Sarkar B, Mitra S, Bhaladhare S (2022) Biochar from biomass: a review on biochar preparation its modification and impact on soil including soil microbiology. Geomicrobiol J 39:373–388. https://doi.org/10.1080/01490451.2022.2028942

Phillips CL, Meyer KM, Garcia-Jaramillo M et al (2022) Towards predicting biochar impacts on plant-available soil nitrogen content. Biochar 4:9. https://doi.org/10.1007/s42773-022-00137-2

Ramamoorthy P, Mary PCN, Bose KSC, et al (2022) Effect of biochar on soil health and crop productivity: a review. Agric Rev. https://doi.org/10.18805/ag.R-2379

Reyhanitabar A, Frahadi E, Ramezanzadeh H, Oustan S (2020) Effect of pyrolysis temperature and feedstock sources on physicochemical characteristics of biochar. J Agric Sci Technol 22(2):547–561

Rodrigues L, Budai A, Elsgaard L et al (2023) The importance of biochar quality and pyrolysis yield for soil carbon sequestration in practice. Eur J Soil Sci 74:e13396. https://doi.org/10.1111/ejss.13396

Romero Millán LM, Sierra Vargas FE, Nzihou A (2021) Characterization of steam gasification biochars from lignocellulosic agrowaste towards soil applications. Waste Biomass Valorization 12:4141–4155. https://doi.org/10.1007/s12649-020-01241-9

Shen Y, Yuan R (2021) Pyrolysis of agroforestry bio-wastes with Calcium/Magnesium oxides or carbonates – Focusing on biochar as soil conditioner. Biomass Bioenergy 155:106277. https://doi.org/10.1016/j.biombioe.2021.106277

Su G, Mohd Zulkifli NW, Ong HC et al (2022) Pyrolysis of oil palm wastes for bioenergy in Malaysia: a review. Renew Sustain Energy Rev 164:112554. https://doi.org/10.1016/j.rser.2022.112554

Tariq R, Mohd Zaifullizan Y, Salema AA et al (2022) Co-pyrolysis and co-combustion of orange peel and biomass blends: Kinetics, thermodynamic, and ANN application. Renew Energy 198:399–414. https://doi.org/10.1016/j.renene.2022.08.049

Tauseef M, Ansari AA, Khoja AH et al (2022) Thermokinetics synergistic effects on co-pyrolysis of coal and rice husk blends for bioenergy production. Fuel 318:123685. https://doi.org/10.1016/j.fuel.2022.123685

Tisserant A, Hu X, Liu Q et al (2023) Biochar and its potential to deliver negative emissions and better soil quality in Europe. Earths Future 11:e2022EF003246. https://doi.org/10.1029/2022EF003246

Tomczyk A, Sokołowska Z, Boguta P (2020) Biochar physicochemical properties: pyrolysis temperature and feedstock kind effects. Rev Environ Sci Biotechnol 19:191–215. https://doi.org/10.1007/s11157-020-09523-3

Tu P, Zhang G, Wei G et al (2022) Influence of pyrolysis temperature on the physicochemical properties of biochars obtained from herbaceous and woody plants. Bioresour Bioprocess 9:131. https://doi.org/10.1186/s40643-022-00618-z

Uddin Monir M, Muntasir Shovon S, Ahamed Akash F et al (2024) Comprehensive characterization and kinetic analysis of coconut shell thermal degradation: energy potential evaluated via the Coats-Redfern method. Case Stud Therm Eng 55:104186. https://doi.org/10.1016/j.csite.2024.104186

Vilas-Boas ACM, Tarelho LAC, Kamali M et al (2021) Biochar from slow pyrolysis of biological sludge from wastewater treatment: characteristics and effect as soil amendment. Biofuels Bioprod Biorefining 15:1054–1072. https://doi.org/10.1002/bbb.2220

Villegas-Pangga G (2020) Production and characterization of biochars from slow pyrolysis of different biomass materials to evaluate properties as soil amendments. Philipp J Sci 150. https://doi.org/10.56899/150.01.25

Wan YK, Sadhukhan J, Ng KS, Ng DKS (2016) Techno-economic evaluations for feasibility of sago-based biorefinery, Part 1: Alternative energy systems. Chem Eng Res des 107:263–279. https://doi.org/10.1016/j.cherd.2015.11.001

Wang L, O'Connor D, Rinklebe J et al (2020) Biochar aging: mechanisms, physicochemical changes, assessment, and implications for field applications. Environ Sci Technol 54:14797–14814. https://doi.org/10.1021/acs.est.0c04033

Wu W, Han J, Gu Y et al (2022) Impact of biochar amendment on soil hydrological properties and crop water use efficiency: a global meta-analysis and structural equation model. GCB Bioenergy 14:657–668. https://doi.org/10.1111/gcbb.12933

Xu H, Cai A, Wu D et al (2021) Effects of biochar application on crop productivity, soil carbon sequestration, and global warming potential controlled by biochar C: N ratio and soil pH: a global meta-analysis. Soil Tillage Res 213:105125. https://doi.org/10.1016/j.still.2021.105125

Xu Q, Wang J, Liu Q et al (2022) Long-term field biochar application for rice production: effects on soil nutrient supply, carbon sequestration. Crop Yield Grain Minerals Agronomy 12:1924. https://doi.org/10.3390/agronomy12081924

Yang H, Yan R, Chen H et al (2007) Characteristics of hemicellulose, cellulose and lignin pyrolysis. Fuel 86:1781–1788. https://doi.org/10.1016/j.fuel.2006.12.013

Yuan S, Tan Z, Zhang L, Huang Q (2021) Study of the Relationship between a nutrient element and two energy elements during the biochar preparation process. Waste Biomass Valorization 12:445–463. https://doi.org/10.1007/s12649-020-00973-y

Zaitun Z, Halim A, Sa'dah Y, Cahyadi R (2022) Surface morphology properties of biochar feedstock for soil amendment. IOP Conf Ser Earth Environ Sci 951:012034. https://doi.org/10.1088/1755-1315/951/1/012034

Zhang X, Zou G, Chu H et al (2023) Biochar applications for treating potentially toxic elements (PTEs) contaminated soils and water: a review. Front Bioeng Biotechnol 11:1258483. https://doi.org/10.3389/fbioe.2023.1258483

Zhao L, Cao X, Mašek O, Zimmerman A (2013) Heterogeneity of biochar properties as a function of feedstock sources and production temperatures. J Hazard Mater 256–257:1–9. https://doi.org/10.1016/j.jhazmat.2013.04.015